Visual Neuroscience (1997), **14**, 691–704. Printed in the USA.

The distribution and morphology of LGN K pathway axons within the layers and CO blobs of owl monkey V1

Y. DING[1] AND V.A. CASAGRANDE[1,2]

[1]Department of Cell Biology, Vanderbilt University, Nashville
[2]Department of Psychology, Vanderbilt University, Nashville

(RECEIVED October 17, 1996; ACCEPTED November 14, 1996)

Abstract

The lateral geniculate nucleus (LGN) of primates contains three classes of relay cells, the magnocellular (M), parvocellular (P), and koniocellular (K) cells. At present, very little is known about either the structure or function of the K relay cells in New or Old World monkeys (simian primates). In monkeys, K cells are located between the main LGN layers and adjacent to the optic tract. For convenience, these intercalated cell layers are numbered K1–K4 starting closest to the optic tract with K1. The objective of this study was to examine the details of K axon morphology in the primary visual cortex (V1) of owl monkeys and to determine if different K layers give rise to distinct axon types. For this purpose, injections of WGA-HRP or PHA-L were made into specific K LGN layers and the distribution and morphology of the resulting labeled axons were analyzed. Injections of fluorescent tracers also were made within the superficial layers of V1 to further document connections *via* analysis of the patterns of retrogradely labeled cells in the LGN. Our main finding is that K axons in owl monkeys terminate as delicate focused arbors within single cytochrome oxidase (CO) blob columns in cortical layer III and within cortical layer I. Overall, the morphology of the K axons in these monkeys is quite similar to what we described previously for K geniculocortical axons in the distantly related bush baby (prosimian primate), suggesting that the basic features of this pathway are common to all primates. Our results also provide evidence that the axon arbors from different K layers are morphologically distinct; axons from LGN layer K1 project mainly to cortical layer I, while axons from LGN layer K3 chiefly terminate in cortical layer III. Taken together, these results imply that the basic features of axons within the K pathway are conserved across primates, and that the K axons from different K layers are likely to differ in function based upon their different morphologies.

Keywords: Striate cortex, Parallel pathways, PHA-L, Primate, Vision

Introduction

In all mammals, including primates, a division of labor occurs at the level of the retina. Separate sets of ganglion cell classes abstract different aspects of the visual image and send signals along parallel pathways. In primates three of these parallel pathways, the magnocellular (M), parvocellular (P), and koniocellular (K) pathways project *via* separate layers of the lateral geniculate nucleus (LGN) to the primary visual cortex (V1) (Casagrande & Kaas, 1994). Since conscious visual perception depends upon an intact V1 in primates, it is assumed that all of the information critical for visual perception is carried *via* one or more of these three parallel channels. However, until relatively recently, little attention has been paid to one of these pathways, namely the K pathway, since it was assumed to be very small, and thus unimportant, in comparison to the M and P pathways (Casagrande, 1994). More recent data have shown that K LGN cells are as numerous as M LGN cells in macaque monkeys (Hendry, 1995). In fact, several aspects of the anatomy, neurochemistry, and physiology of the K pathway to V1 in different primate species indicate that this pathway could play an important role in vision (see Casagrande, 1994 for discussion).

To date, the most detailed studies of K LGN cells have been in the prosimian primate, bush baby. In this species, physiological studies have suggested that K cells are a heterogeneous population that share some features with cat LGN W-cells (Norton & Casagrande, 1982; Irvin et al., 1986; Norton et al., 1988). Neurochemically, K LGN cells in bush babies are distinct in that they are the only cells in the LGN containing the calcium-binding protein, calbindin (Diamond et al., 1993; Johnson & Casagrande, 1995). K LGN cells in bush babies are also distinct from P and M cells in their projections to V1; K axons terminate directly within single cytochrome oxidase (CO) blobs within layer IIIB and more broadly within layer I, while M and P axons terminate within layer IV (Lachica & Casagrande, 1992).

In simian primates, the cells belonging to the LGN K pathway are difficult to study due to the fact that these cells are more scattered between and below the more densely packed cells within the M and P layers (Kaas et al., 1978). Nevertheless, many of the characteristics of K LGN cells identified for bush babies also appear as signature characteristics for this pathway in simian pri-

Reprint requests to: V.A. Casagrande, Department of Cell Biology, Vanderbilt Medical School, Medical Center North RM C2310, Nashville, TN 37232-2175, USA.

mates. As in prosimians, K cells in simians are neurochemically distinct and contain calbindin (Jones & Hendry, 1989; Johnson & Casagrande, 1993). Also as in bush babies, data from bulk labeling studies of LGN pathways of owl monkeys, squirrel monkeys, and macaque monkeys indicate that the K cells provide the main, perhaps the sole, direct LGN input to the supragranular layers of V1 terminating within the CO blobs of cortical layer IIIB and in layer I (Livingstone & Hubel, 1982; Fitzpatrick et al., 1983; Weber et al., 1983; Diamond et al., 1985; Hendry & Yoshioka, 1994).

In spite of the fact that common features can be found that define K cells across primates, there is also evidence of differences. Anatomically, the relative concentration of K cells within the different interlaminar zones of the LGN, as defined by calbindin immunocytochemistry, shows considerable interspecies variability (Hendry & Casagrande, 1996). The retinal and superior collicular axons that project to K cells in bush babies are heterogeneous (Lachica & Casagrande, 1993), as are the receptive-field properties of K cells (Norton & Casagrande, 1982; Irvin et al., 1986; Norton et al., 1988). Additionally, data in both squirrel monkeys and macaque monkeys indicate that different populations of LGN K cells may project to different supragranular layers of V1, at least based upon bulk labeling of different subsets of layers in the LGN or of cortex (Fitzpatrick et al., 1983; Weber et al., 1983; Hendry & Yoshioka, 1994). Several investigators also have reported that a subset of K LGN cells in simians projects to extrastriate visual areas including V2, MT and inferior temporal cortex (ITC) (Benevento & Yoshida, 1981; Bullier & Kennedy, 1983; Kennedy & Bullier, 1985; Lysakowski et al., 1988; Hernandez-Gonzalez et al., 1994). Thus, there is evidence to suggest both that the K pathway may differ across primates and that this pathway may actually consist of more than one subpathway.

In light of the above, our main objective was to characterize, in detail, the morphology of K LGN axons in a simian primate. Additionally, we wished to determine if K geniculocortical axons in simians are similar to or different from what has been described in prosimians. A final goal was to determine if K cells located in different layers in the LGN have morphologically distinct axon arbors within V1 or axon arbors that project to extrastriate areas.

Methods

Six adult owl monkeys (*Aotus trivirgatus*) were used in the present study. Three of these animals were employed to examine the overall distribution of K cell projections to V1. This analysis involved either anterograde labeling of axons *via* LGN injections of wheat germ agglutinin conjugated to horseradish peroxidase (WGA-HRP) or retrograde labeling of the K LGN cells *via* fluorescent dextran or Fast Blue injections into V1. Three additional monkeys were used to demonstrate the detailed structure of individual K cell axons by injections of the kidney bean lectin *Phaseolus vulgaris leucoagglutinin* (PHA-L). All of the animals were cared for according to the *National Institutes of Health Guide for the Care and Use of Laboratory Animals* and the guidelines of the Vanderbilt University Animal Care Committee.

Surgical procedures

All surgical procedures were carried out under aseptic conditions. Prior to surgery, atropine sulfate (0.1 mg/kg) was given to inhibit salivation. The owl monkeys then were intubated, anesthetized with isofluorane (3–4%) in oxygen, and maintained with the same gas mixture at 1–2%. Heart and respiration rates were continuously monitored and reflexes tested periodically; animals also were kept warm with a water circulating heating pad throughout surgery. Postoperatively, all animals were given 0.02 mg/kg of Banamine as an analgesic and 300,000 units/kg of a long acting penicillin (Flocillin) and monitored carefully until they were fully conscious and capable of eating and drinking on their own. At that point, they were returned to their home cages and provided with soft palatable foods and water. Details of the surgery were similar to those described earlier (Lachica & Casagrande, 1992).

Labeling K LGN cell axons

Once deeply anesthetized, the monkeys were secured in a stereotaxic apparatus, the skull exposed, and a bilateral craniotomy performed. A dural flap was elevated and 5% Agar in saline was spread over the pial surface to prevent desiccation. The LGN layers were identified by recording visually evoked responses to a flashing light through an electrode glued to a pipette filled with tracer (1% WGA-HRP in saline or 4% PHA-L in 0.05 M phosphate buffer, pH 7.4). When the appropriate K layer was identified on the basis of changes in eye dominance, tracers were iontophoretically injected for either 30 min for the WGA-HRP injections (3 s ON/3 s OFF, 3–5 μA), or 20–40 min for the PHA-L injections (7 s ON/7 s OFF, 1–3 μA). When the injections were completed in both hemispheres, the dural flap was repositioned, and the skin was sutured.

Retrograde labeling of LGN K cells

To label the most superficially projecting K axons, one owl monkey received deposits of different fluorescent tracers in each hemisphere. The dura and pia were removed on one side and 5% Fast Blue in saline was distributed on the surface of the brain and left for 50 min before rinsing off with saline. This procedure resulted in label restricted to cortical layers I, II, and the upper portion of layer III (IIIA). After depositing the label, the dura and pia were repositioned. In the other hemisphere, 5% fluorescein isothiocyanate (FITC)-dextran was injected into cortical layer IIIB/IIIC after removing the dura. When the surgery was complete the animal was treated as described above for the other animals.

Histological procedures

After a 2-day (WGA-HRP cases), 7–21 day (PHA-L cases), or 13-day (fluorescent tracers case) survival, the animals were anesthetized deeply with an overdose of Nembutal. The animals that had received WGA-HRP or fluorescent tracer injections were initially perfused transcardially with a brief rinse of saline, then perfused with 2–4% paraformaldehyde in 0.1 M phosphate buffer (pH 7.4), and finally perfused with 10% sucrose in the same fixative. The PHA-L-injected animals were perfused the same way except that the fixative contained 2% paraformaldehyde/0.1% glutaraldehyde/0.2% picric acid in 0.1 M phosphate buffer (pH 7.4) and the sucrose/fixative rinse was followed by a final rinse with 0.05 M phosphate buffer, pH 7.4. All brains were stored in 30% sucrose buffer overnight at 4°C. In the two cases with WGA-HRP injections, one hemisphere of cortex was gently unfolded and flattened between glass slides. The flattened tissue was immersed in 30% sucrose buffer overnight at 4°C. The LGNs and all but two hemispheres of cortex were frozen and sectioned parasagittally at 52 μm. The two flattened hemispheres were cut tangentially at the same thickness.

WGA-HRP histochemistry

A sensitive low artifact TMB procedure (Gibson et al., 1984) was used for the demonstration of WGA-HRP on alternate sections. Every fourth parasagittal section was stained with Neutral Red to identify the LGN and cortical layers. Every second tangential section from the flattened cortices was treated to show CO blobs (Wong-Riley, 1979). All sections were mounted on gelatin-coated slides, air dried, dipped briefly in a clearing agent (Histo-Clear), and coverslipped.

PHA-L immunocytochemistry

LGN and cortical sections were incubated for 24–48 h in Tris-buffered saline (TBS) containing 2% normal rabbit serum and an antibody raised against PHA-L (Vector Labs, Burlingame, CA) at a 1:2000 dilution. The tissue was then incubated for 2 h in linking antibody (biotinylated rabbit anti-goat) at a 1:200 dilution. Sections were then developed with diaminobenzidine (DAB) as a chromogen with nickel-enhanced glucose oxidase (Sawchenko et al., 1990). In two cases, every third section was also stained for CO (Wong-Riley, 1979). In one case, every second section was stained for Nissl bodies to confirm cortical and LGN layers.

Fluorescent tracers

The sections of thalamus and cortex from the brain injected with Fast Blue and fluorescein isothiocyanate (FITC)-dextran were mounted on glass slides and coverslipped with phosphate buffer, pH 7.4. The sections were examined and photographed immediately using a Zeiss fluorescence microscope with excitation filters of 365-nm and 450–490-nm wavelengths, respectively. The sections were then removed and mounted on gelatinized slides and stained for Nissl bodies.

Reconstruction and analysis

All LGN injection sites were reconstructed from serial sections using a microprojector at low magnification (170×) to document the location and extent of the label. The cortical injections were reconstructed from photographs taken of sections through the full extent of the labeled area.

Within the tangential cortical sections, the bulk distribution of geniculocortical projections resulting from the WGA-HRP injections in LGN was reconstructed and superimposed on a plot of the location of CO blobs using a *camera lucida* drawing tube at a magnification of 60×. Matching blood vessels and section artifacts were used as fiduciary points for aligning the sections.

The distributions of retrogradely labeled cells in the LGN layers following fluorescent tracer injections in the cortex were reconstructed in relationship to the LGN layers by first observing and photographing all labeled cells throughout the LGN and then aligning the label in these photographs with the boundaries of the LGN layers obtained by subsequent Nissl staining of the same sections.

Individual axons and axon arbors were reconstructed at a total magnification of 1000× with the aid of a *camera lucida*. Only axons that showed clear filling of terminal branches were chosen for reconstruction. Whole arbors were traced through successive sections to ensure that all branches of the arbor were included. We are quite confident that complete arbors were reconstructed since we generally found the ends of branches with boutons. We rarely found labeled axons that fade off gradually. In the present study, the cortical laminar borders were revealed initially by a combination of the heavy metal intensification step and CO staining, and finally confirmed by Nissl counterstaining.

For each axon arbor the anterior-posterior (A-P) and medial-lateral (M-L) diameter at its widest point, the ratio of the A-P/M-L diameters, the total number of and relative density of boutons, and the percentage of the arbor and number of boutons within each layer were also measured. The A-P diameter of the arbor is defined here as the spread of the arbor running parallel to the layer along a line from the most anterior tip to the posterior tip. The M-L width was estimated by the thickness of the sections through which the arbor extended. The total extent of the arbor was calculated as a linear measure by tracing the full extent of the axon and all its branches. The percentage of branch length found in the different layers was used to demonstrate the level of arbor communication within each layer. Bouton density was defined as the total bouton number divided by arbor branch length. Bouton density in each layer and sublayer also was measured relative to the length of arbors in different layers obtained as described previously. All measurements were made with the aid of the BioQuant-IV image analysis system (R&M Biometric Inc., Nashville, TN).

Results

Our results provide clear evidence in owl monkeys that individual K LGN axons terminate principally within single CO blobs in layer III and in layer I. Interestingly, axons arising from K cells located in the principal interlaminar zone between the magnocellular and parvocellular layers (layer K3) terminate mainly within the centers of single CO blobs in cortical layer IIIBα, whereas axons arising from K cells adjacent to the optic tract (layer K1) terminate principally in cortical layer I and IIIA above the center of a CO blob. These findings suggest that different LGN K layers make distinct contributions to V1. Below we consider these findings in more detail beginning with a description of the LGN and V1 cortical layers in the owl monkey.

Defining layers

Before presenting our main findings, it is necessary to define briefly the terms we have chosen to describe the LGN and cortical layers in owl monkey. Several terminologies have been used to describe the different layers of the LGN in different primate species. Fig. 1 is a photomicrograph showing our interpretation of layer boundaries in owl monkey LGN as viewed in a Nissl-stained parasagittal section. The most common way of designating primate LGN layers has been to number them from the optic tract starting with the first magnocellular layer as layer 1 (Kaas et al., 1978). This numbering scheme has two problems. First, although all primates exhibit a standard set of two parvocellular (P) layers and two magnocellular (M) layers within regions of the nucleus representing the visual periphery, each P layer can split into two or more layers (typically 2) in the region of the nucleus representing central vision. Second, all primates exhibit small-celled layers between the main layers and adjacent to the optic tract that have not typically been included in this numbering scheme. The latter have been given a variety of names depending upon their position in the nucleus. The cell group(s) next to the optic tract has been referred to as the "0" or "superficial S" layer or layers (Chacko, 1955; Campos-Ortega & Hayhow, 1970; Giolli & Tigges, 1970; Kaas et al., 1978). The smallest cells that lie between the ipsilaterally innervated M and P layers have been referred to as the intercalated layers (Fitzpatrick

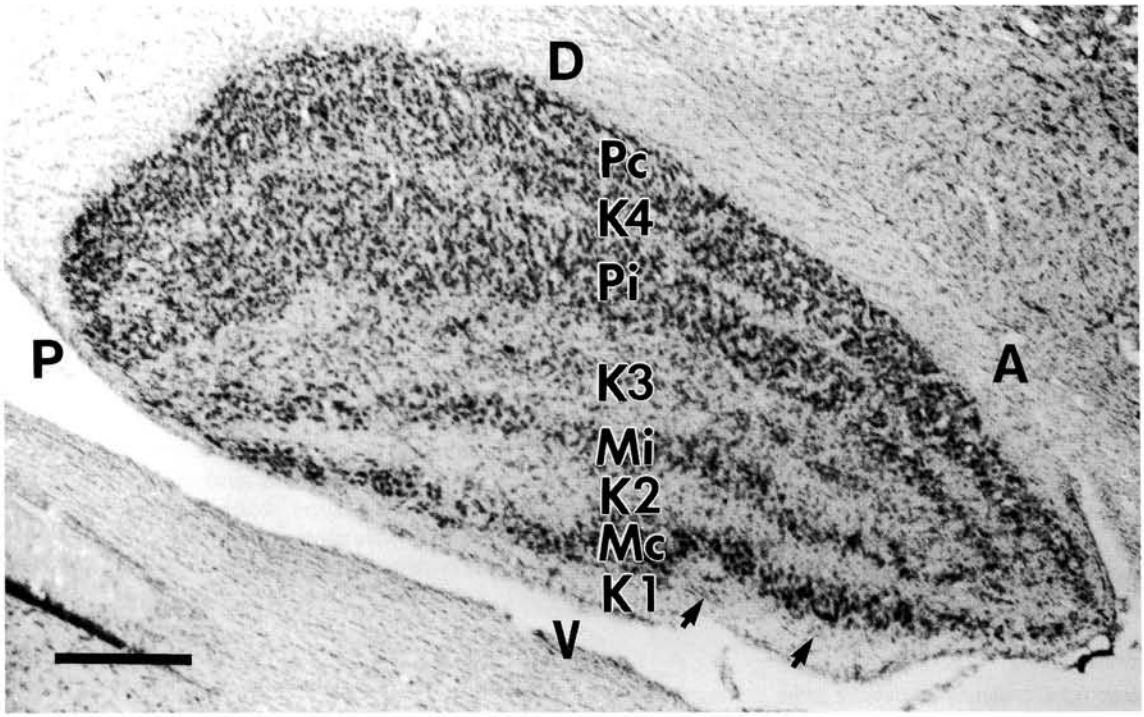

Fig. 1. A Nissl-stained parasagittal section [anterior (A) toward the right and dorsal (D) toward the top] showing the LGN layers in owl monkey. The Koniocellular, Magnocellular, and Parvocellular layer are designated K, M, and P, respectively. The K layers lie between the main LGN layers and next to the optic tract and are numbered from 1 to 4 beginning at the optic tract. Arrows indicate cells in K1. c, innervated by the contralateral eye; i, innervated by the ipsilateral eye; P, posterior; V, ventral. Scale bar = 500 μm.

et al., 1983). In prosimians the small-cell layers between the two P layers have been called the Koniocellular layers (dust-like layers in reference to the small size of cells) (Kaas et al., 1978). Most recently, Casagrande (1994) has used the designation Koniocellular (K) to refer to all these small cells regardless of position in the nucleus. For convenience, we have adopted a modification of this terminology as follows. The two P layers of the owl monkey are designated P_c and P_i to distinguish the P layers by ocular input (P_c, contralateral; P_i, ipsilateral). The M layers are designated in the same manner. Since there is controversy over the ocular input and number of the small-cell layers (see Fitzpatrick et al., 1983), we have followed the suggestion of Hendry and Casagrande (1996), and defined all cell groups/layers lying outside of the main layers as K cell layers, numbering them starting from the optic tract as K1 (the S or 0 layer), K2 (between the M layers), K3 (the intercalated layers between the M and P layer), and K4 (between the two P layers).

In V1, differences in interpretation of laminar borders and in naming layers have also caused confusion. Thus, it is important, for comparison with the results of others, to provide clear definitions. Fig. 2 is a photomicrograph showing our interpretation of layer boundaries in V1 as viewed in a Nissl-stained section. We have used Fitzpatrick et al.'s (1983) modification of the nomenclature originally proposed by Hässler (1967) (see also Casagrande & Kaas, 1994 and Boyd et al., 1997 for discussion). Brodmann's (1909) nomenclature is indicated in parentheses for comparison (if different). The main differences in interpretation concern the sublayers above layer IV (IVC of Brodmann). Layer III in the owl monkey, as in other primates, can be divided into three distinct layers. Layer IIIA is identified by its more sparse cell distribution in comparison to cell dense layer II. The cells of layer IIIBα are more closely packed than in layer IIIA. The border between layer IIIA and IIIBα is often marked by a row of relatively large pyramidal cells. IIIBβ can be recognized as a granular tier of cells at the base of IIIBα. Since owl monkeys, unlike some simians, do not have direct P LGN input that lies above layer IV (Kaas et al., 1976), one cannot use a CO stain to identify IVA as defined in macaque monkeys by Lund (1988) using Brodmann's nomenclature. A comparable sublayer to IVA in macaque monkeys would likely lie at the base of what we have termed IIIBβ. Layer IIIC has two parts, a more cell-sparse part and a lower part containing many very large pyramidal cells. These very large cells provide a useful landmark for the IIIC/IVα border as also described by Fitzpatrick et al. (1983) for squirrel monkey V1.

The overall pattern of K layer projections

The general pattern of geniculocortical projections from the individual layers of the LGN in owl monkeys was reported by Diamond et al. (1985). Their results showed that, as in other primates, the M layers project to cortical layer IVα, the P layers project to IVβ, and the proposed intercalated (K) geniculate layers project above layer IV. A large injection of WGA-HRP that involved all of the LGN layers confirms this original pattern reported by Diamond et al. (1985). Fig. 3 shows a plot of terminations in V1 following such an injection. A dense continuous band of label is clearly evident in layer IV. In fact, due presumably to a slightly uneven spread of the injection within the layers of the LGN, a clear line is evident in layer IV that appears to mark the boundary between the terminations of the P and M LGN layers to cortical sublayers IVα and IVβ, respectively. Above layer IV distinct patchy label is seen focused within layer IIIB with a center to center spacing of ap-

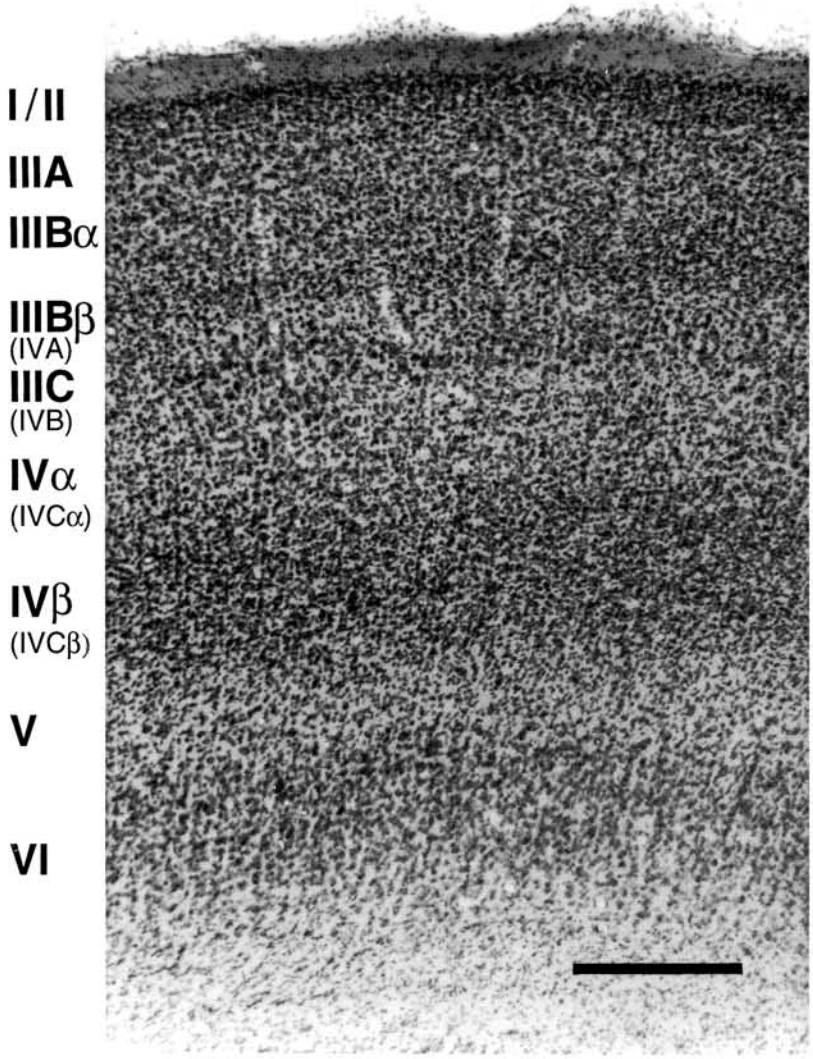

Fig. 2. A Nissl-stained parasagittal section showing the V1 layers in owl monkey. Roman numerals refer to the cortical layers. We use a modification of the nomenclature originally proposed by Hässler (1967). Brodmann's (1909) laminar designations are given in parentheses (if different). Scale bar = 250 μm.

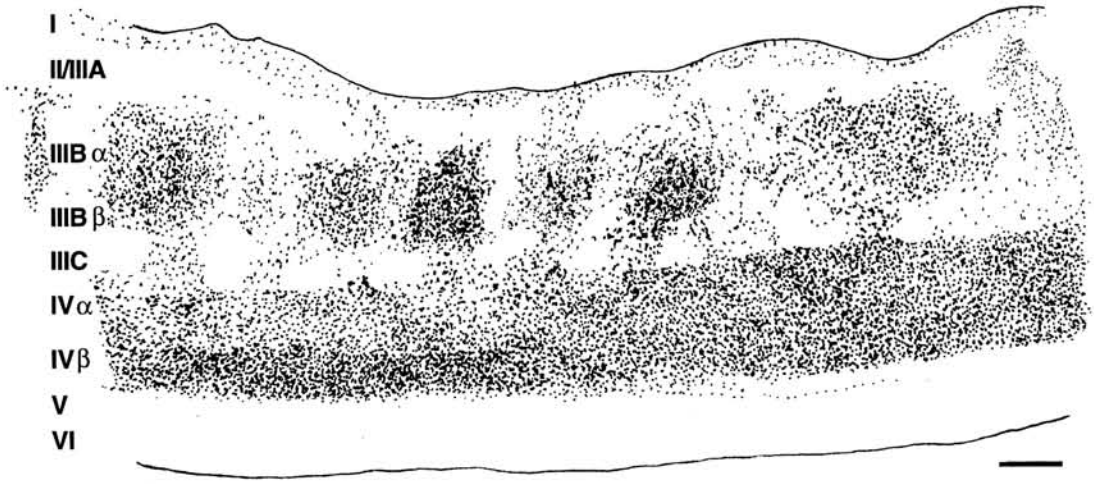

Fig. 3. A plot of the terminal label from a single parasagittal section through V1 following a large injection of WGA-HRP that involved all of the LGN layers. Note that the most dense label is found in layers IV and IIIBα, with less dense patches of label in the other supragranular layers and a continuous band of label in layer I. Other conventions are as in Fig. 2. See text for details. Scale bar = 200 μm.

proximately 360 μm. Lighter patchy label appears to extend also into IIIA and IIIC. Superficially, a light continuous band of label is seen in layer I.

In another case, we examined the distribution of the patchy K LGN projections to layer IIIBα in tangential sections and compared this distribution of label with the distribution of CO blobs on adjacent CO-stained sections (see Figs. 4A and 4B). The patchy white pattern of label seen in Fig. 4A resulted from an injection centered within LGN layer K3. This label appears to colocalize with the CO blobs. Fig. 4B shows a plot of the distribution of label within cortical layer IIIBα (shown in Fig. 4A) superimposed on a plot of CO blobs drawn from an adjacent section. It is obvious from these plots that virtually every patch of label is aligned with a CO blob, although the K terminal patches appear, in most cases, to extend slightly beyond the blob borders.

The total pattern of LGN projections to V1 can be contrasted to the pattern seen following a WGA-HRP injection confined to the dorsal portion of the LGN including both P layers, and K4 and K3. As seen in Fig. 5, the terminations are now confined principally to IVβ and IIIB with few if any terminals visible in layer I. This pattern of terminations suggested to us that layer I might receive projections principally from the K layers below K3. Since few cells in owl monkeys are located within LGN layer K2, the likely origin of the projection to cortical layer I is LGN layer K1.

To confirm this finding, we made restricted injections of fluorescent tracers either aimed at layer I or layer III of the visual cortex, respectively, in order to determine if different subsets of K cells projected to these cortical layers. With an injection of Fast Blue centered in layer I extending only as far as the top of layer IIIA, cells in all of the K layers, except K4, were labeled (see

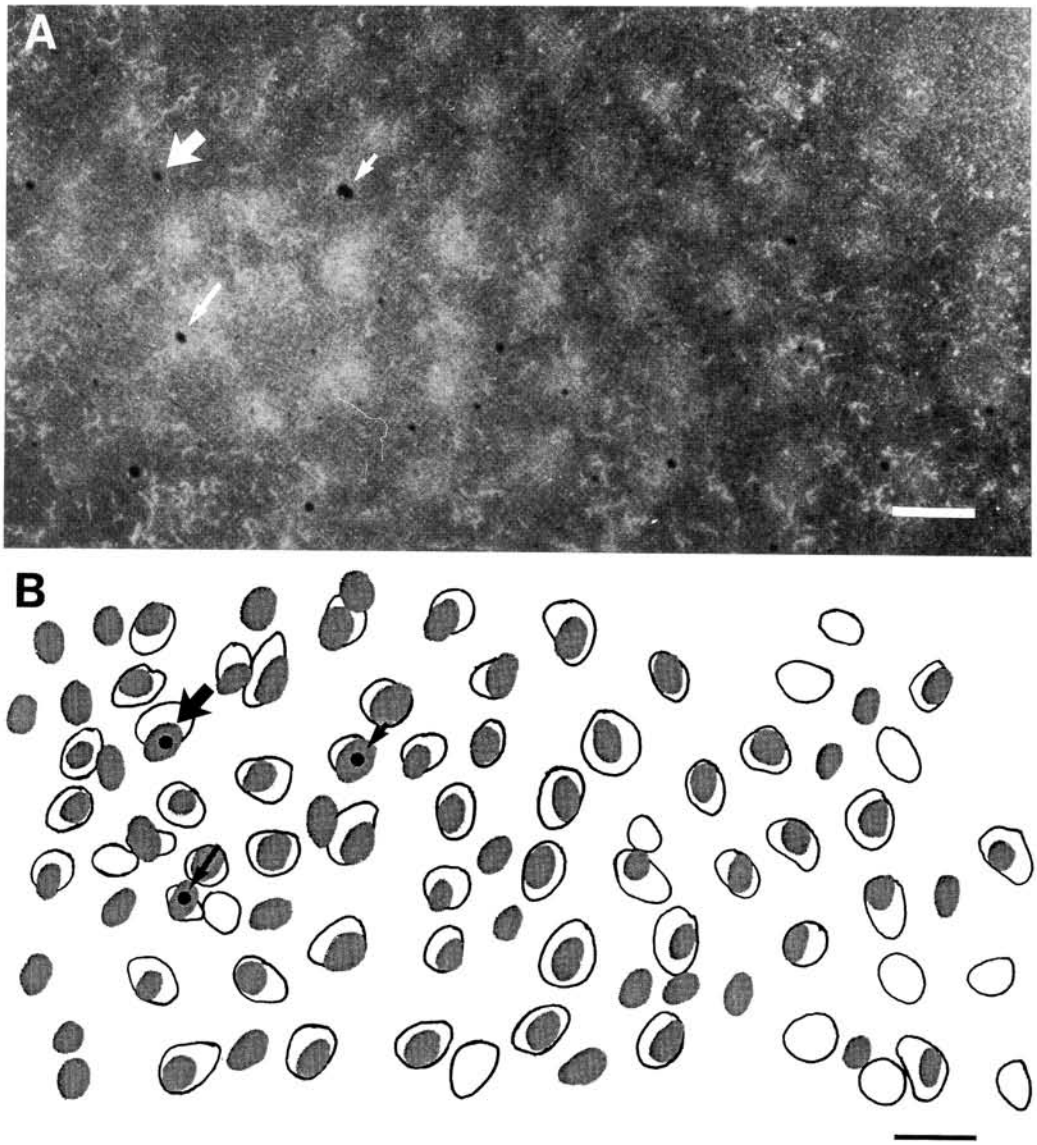

Fig. 4. The distribution of terminal label within a tangential section through layer IIIBα of V1 following a large LGN injection centered in K3 is shown. (A) A dark-field photomicrograph of the terminal label seen as white patches in IIIBα. (B) A plot of the above background label (outlines) in relationship to the location of CO blobs (gray patches). Common blood vessels (indicated by white arrows in A and black arrows in B) were used to align sections. Note that the terminal label is confined principally to CO blobs. Scale bars = 500 μm.

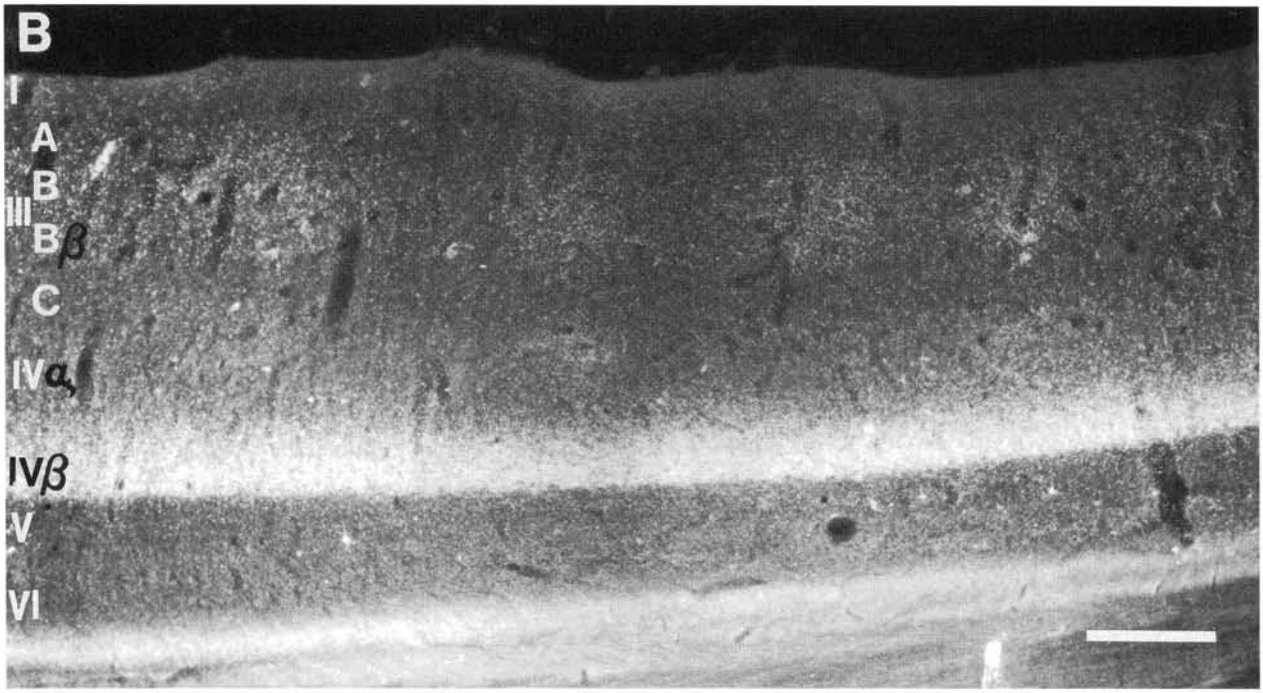

Fig. 5. A dark-field photomicrograph of the terminal label (white) in V1 following a WGA-HRP injection confined to the dorsal portion of the LGN including both P layers, and also layers K4 and K3. Roman numerals refer to the cortical layers. Other conventions are as in Fig. 2. Scale bar = 200 μm.

Fig. 6A). However, when deposits of FITC-dextran were centered in cortical layer IIIB with no involvement of layer I, all of the K layers were labeled except layer K1 (see Figs. 6B and 6C). These data, combined with the anterograde tracing experiment, indicate that K4 projects to layer IIIB but does not project to I while K1 shows the reverse pattern. It is unclear from our bulk labeling data whether K2 and K3 exhibit differences in cortical laminar projections since cells in both of these layers were retrogradely labeled *via* either the layer I–IIIA injection or the IIIB/IIIC injection. To resolve this issue further, we labeled and reconstructed individual K axons, the results of which are described next.

Morphology of individual K axons

We examined and compared details of individual K axon arbors labeled by PHA-L *via* injections aimed at layers K3 or K1 of the LGN. All arbors were plotted in relationship to CO blobs identified on every third section. As predicted from our bulk labeling results, all individual K axons labeled by these injections terminated either within a CO blob or directly above or below a CO blob in V1.

K3 axon arbors

Small injections of PHA-L were made into K3. Fig. 7 shows a bright-field photomontage of a representative K3 axon reconstructed following an injection centered in layer K3 and involving the adjacent P and M layers. This axon was one of 13 K3 axons reconstructed from the white matter through all cortical layers. This axon can be seen to branch repeatedly within cortical layer IIIBα with multiple boutons *en-passage*.

K3 geniculocortical axon arbors showed branches in different layers and sublayers. Examples of these different branching patterns are numbered 1–4 in Fig. 8. All of these K axons give rise to complex focused terminations in layer IIIBα composed of very fine branches and, in some cases, much less complex branches in layer I, the latter arise from a collateral of the parent axon. Some axons have terminations that extend into layers IIIA and IIIBβ. A few arbors have branches with terminations in layer IIIC. The branches of the latter K axons bifurcate to produce sparse bouton-bearing telodendria, which are confined within the same CO blob column as the main part of the arbor located in layer IIIBα. A few axons with main arbors in layer III also have simple branches in layer V or tiny branches in layer IVα.

In one case, we also recovered a single arbor in V2 following a K3 injection (arbor #5 in Fig. 8). This V2 arbor is distinct in morphology from any of the K arbors reconstructed in V1 and has elongated main branches with a number of short side branches terminating only in the bottom of layer III and layer V.

Quantitative measures of the K3 terminal arbors showed that these axons are quite restricted averaging 227 μm $\pm$ 49 SE with a range of 100–300 μm in maximum diameter. The most noteworthy feature of these arbors is that they always appear to confine their branches to a CO blob column even if the branches extend into layers above or below the center of the blob.

Another way to examine the extent of these arbors is to compare their terminal distribution to the map of the visual field in V1. The A-P length of the arbor defines the spread of the arbor running parallel to or oblique to the horizontal meridian along a central to peripheral visuotopic axis (Allman & Kaas, 1971). The M-L width defines the spread of the arbor roughly along a visuotopic azimuth. The ratio of A-P/M-L was used as an index of relative isotropy. All terminal arbors were found to be anisotropic (average ratios of 2.3) with the long axis running along the A-P dimension. Without more data from different retinotopic locations (all arbors reconstructed

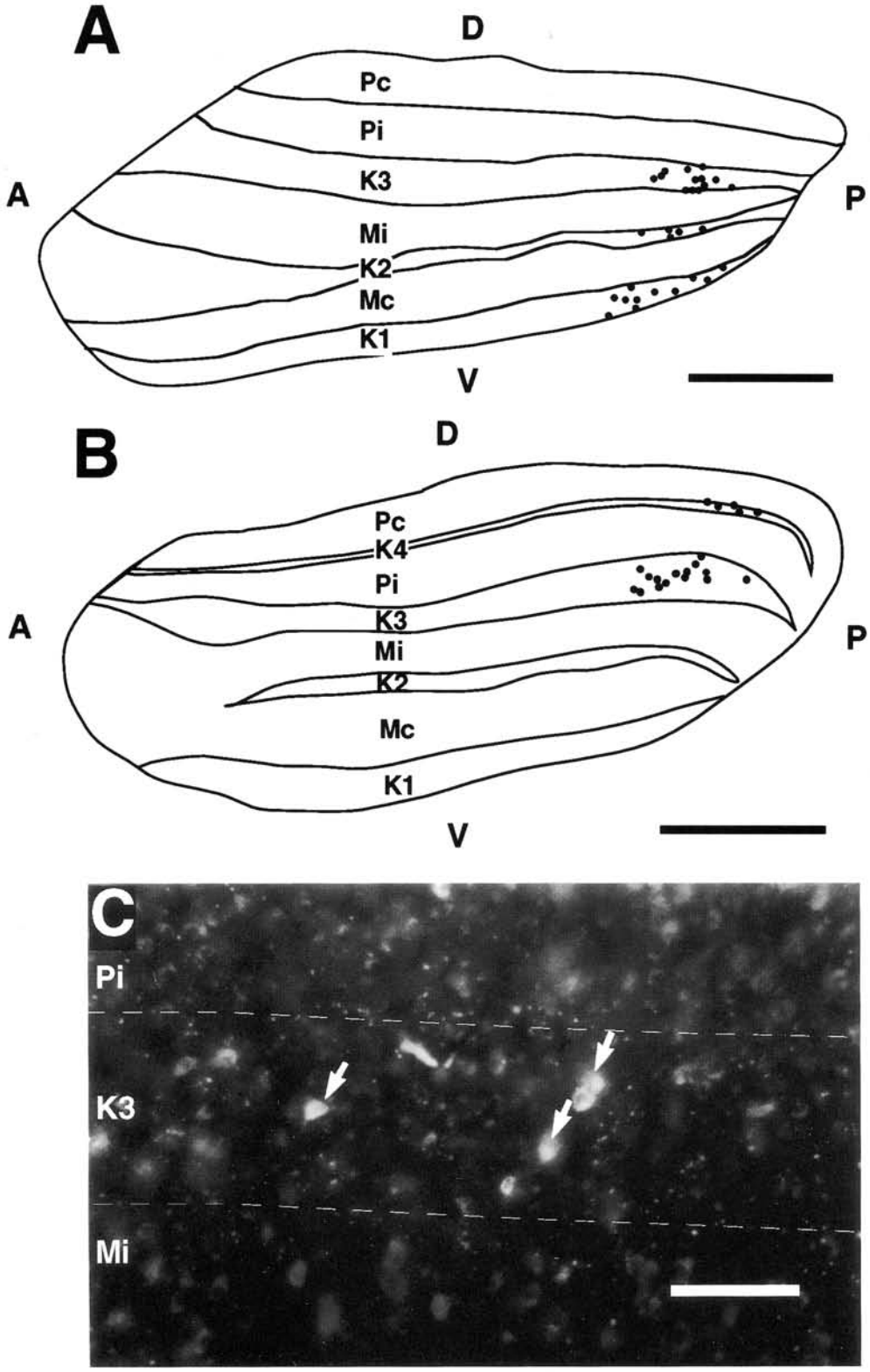

Fig. 6. A comparison of the reconstructed distribution of retrogradely labeled cells in the LGN K layers following an injection of Fast Blue centered in cortical layer I extending only as far as the top of layer IIIA (A), with the reconstructed distribution of retrogradely labeled cells in the LGN K layers following deposits of FITC-dextran in cortical layer IIIB with no involvement of layer I (B,C). In A and B, the retrogradely labeled cells, indicated by black dots, were reconstructed through several sections. C shows the appearance of the labeled cells from a single section from the series used to reconstruct the drawing shown in B. Note that following the more superficial cortical injection cells in all of the K layers except K4 are labeled (A) whereas following the deeper cortical injection cells in all of the K layers except K1 and K2 are labeled (B). Anterior (A) toward the left and dorsal (D) toward the top. Other conventions are as in Fig. 1. Scale bars in: A = 500 μm, B = 500 μm, and C = 100 μm.

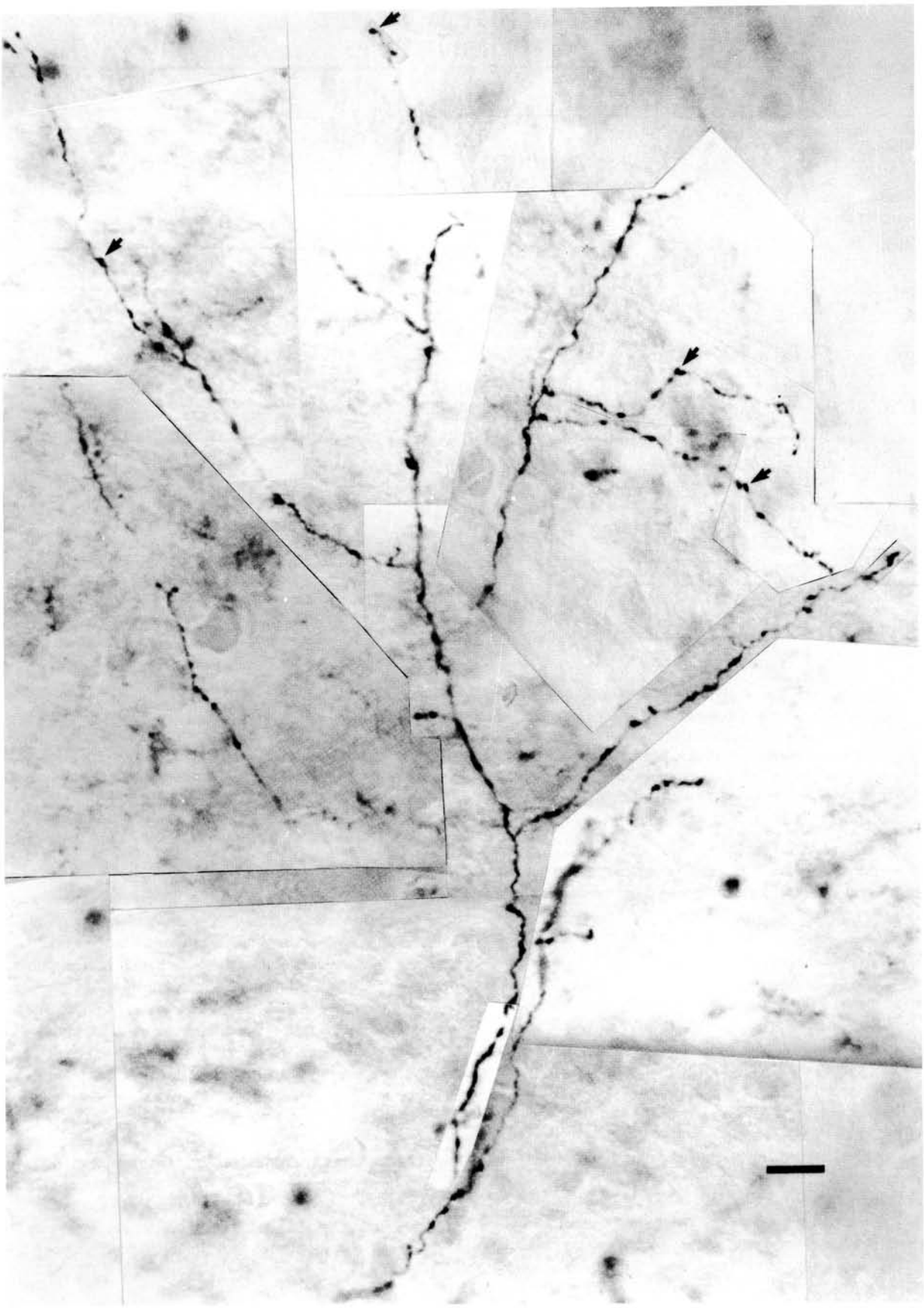

Fig. 7. A photomontage through the branches and boutons (examples are indicated by arrows) of a representative K axon following a small injection of PHA-L made into LGN layer K3. Scale bar = 10 μm.

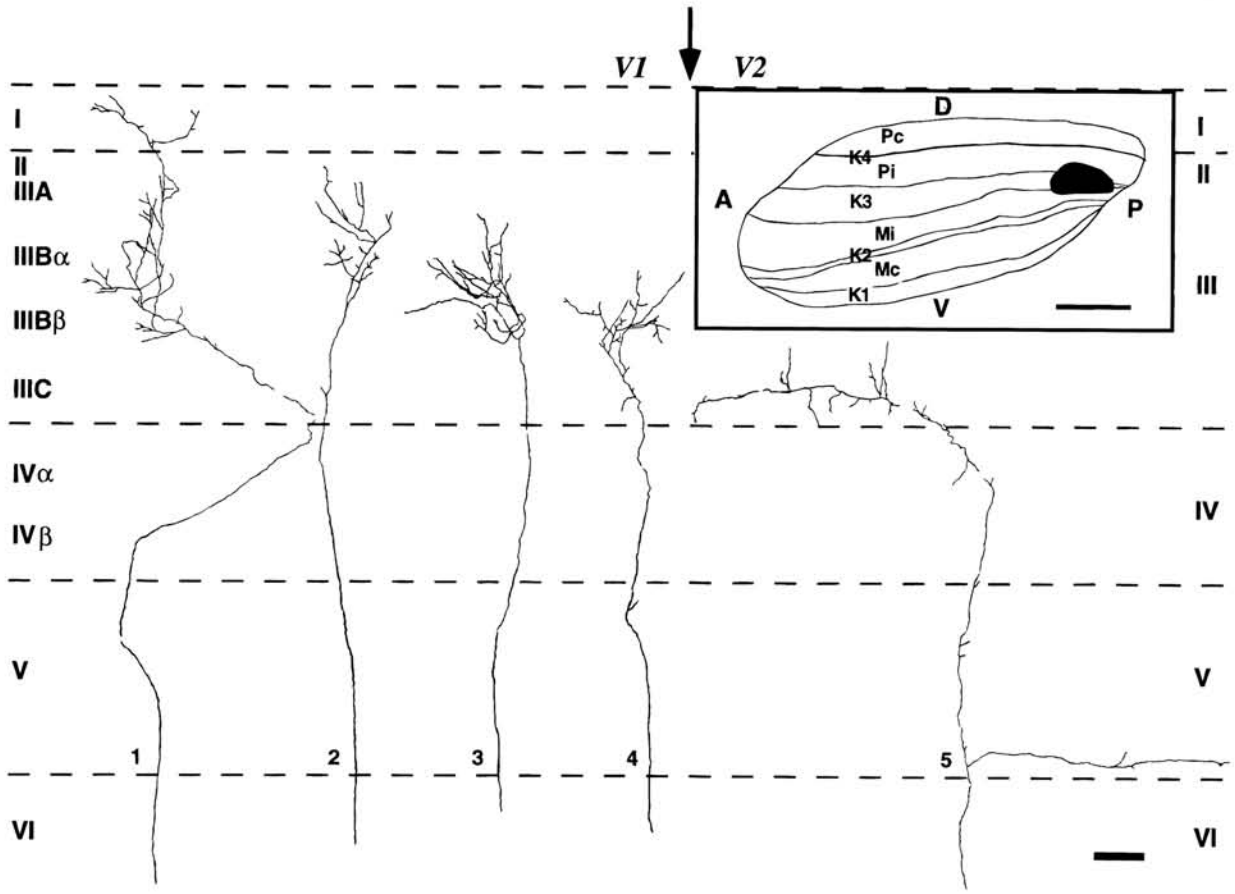

Fig. 8. Reconstructions of five different patterns of axon branching found following an injection of PHA-L into K3 (insert). Axons 1–4 are within V1 (left of the arrow). All V1 axons have terminal branches in IIIBα and all terminate above layer IV but show differences in their termination patterns within the other supragranular layers. Axon 5 was found in V2 (right of the arrow). This V2 axon exhibits a distinct morphology terminating mainly in the bottom of layer III and layer V. Roman numerals indicate cortical layers. The laminar organization of V1 and V2 is given separately on right and left of the figure. In the insert the extent of the injection site is indicated in black. Other conventions are as in Figs. 1 and 2. Scale bar = 100 μm. For the insert, scale bar = 500 μm.

were from the posterior pole of V1), it is unclear exactly how these anisotropies relate to the visuotopic map in owl monkey (Allman & Kaas, 1971).

Since the K3 arbors typically terminate in more than one cortical layer, we wished to examine the proportion of each arbor and the percentage of the total number of boutons within each cortical layer. The majority of the branches (57%) of these arbors is found in layer IIIBα, with 2% in layer I, 10% in layer IIIA, 26% in IIIBβ, and 5% in IIIC. Not surprisingly, the percentage of boutons within each of the layers roughly matches the arbor branch distribution. Thus, the majority (55%) of boutons is found in layer IIIBα, with a minority 3% in layer I, 11% in IIIA, 26% in IIIBβ, and 5% in layer IIIC. There are 5 boutons per 100 μm length of axon, on average, with 6/100 μm in layer IIIBα and 4/100 μm in other layers, respectively.

In summary (Fig. 9), 8% of all axons analyzed terminate only in layer IIIBα and the majority (77%) of the axons arborizes mainly in layer IIIBα. All of the axons appear to be confined to CO blob zones. The axons with main branches in IIIBα also arborize in layer IIIBβ (70%) and IIIA (60%). Only 30% of the arbors have terminal branches in layer I. The same percentage also exhibits a single branch in IVα with 15% showing a single branch below IVα within layer V.

K1 axon arbors

Eight individual K1 layer geniculocortical axons were completely reconstructed from the white matter through all cortical layers following a small injection into layer K1 of the LGN. K1 axons are much simpler in morphology than K3 axons with branches mainly confined to layer I. Four examples of the different morphologies seen among K1 axons are shown in Fig. 10. The terminal branches of K1 arbors are restricted to an area averaging 81 μm $\pm$ 60 SE in diameter (range 25–195 μm). Sixty-three percent of the arbors are distributed over an area of less than 100 μm in diameter. These restricted arbors also appear to be confined to a CO blob column with branches confined either to layer IIIA (19%) or layer I (81%), above the CO blobs in IIIBα (see Fig. 11).

As predicted from the branch pattern, the majority (75%) of arbor boutons are seen in layer I, with the remainder in layer IIIA. No branches are found in layer II. The mean number of boutons/branch segment for these K1 layer arbors is low with only 4/100 μm in both layers I and IIIA.

Discussion

Our results are significant for two reasons. They provide the first detailed description of the V1 axon arbor morphology of K LGN

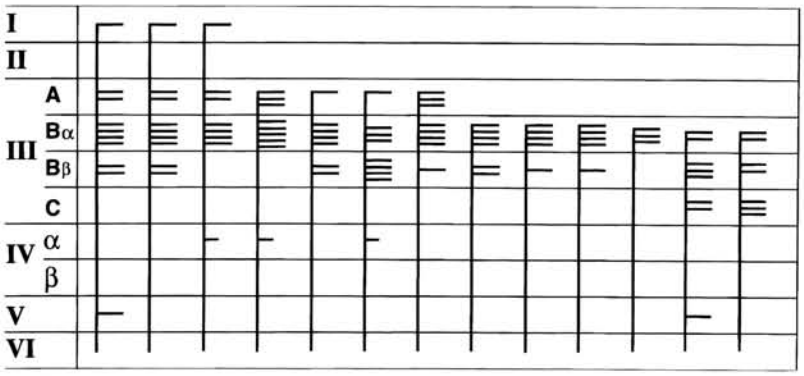

Fig. 9. A schematic diagram summarizing the branching patterns of all 13 V1 axons reconstructed following LGN injections centered in layer K3. The number and length of bars are not intended to represent exact branch length, but to give a general idea of branch density within each layer. The shorter bars indicate branches in which no boutons were visible. Roman numbers indicate cortical layers.

pathway cells in any simian primate. K axons in owl monkeys terminate as small arbors within single CO blob columns in cortical layer III and within cortical layer I. Overall, the morphology of the K geniculocortical axons of owl monkeys is quite similar to what we described previously for K geniculo-cortical axons in bush babies, in which the K LGN axons end as single complex arbors within one CO blob column in layer III with a collateral in layer I (Lachica & Casagrande, 1992). This similarity suggests that the basic features of this pathway are common to all primates. Additionally, our results provide evidence that axons arising from different K LGN layers in owl monkeys, although they share features in common, also are morphologically distinct. Below we consider the interpretation of these findings in light of past work in the field.

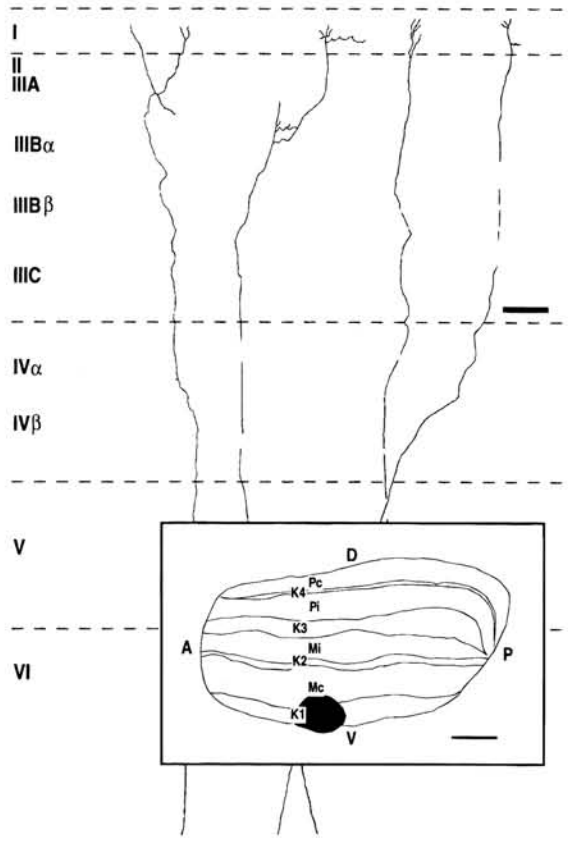

Fig. 10. Reconstructions of four different axons found following an injection of PHA-L into K1 (insert). All axons have terminal branches in layer I with two having branches below this layer in layer IIIA. Roman numerals indicate cortical layers. In the insert the extent of the injection site is indicated in black. Other conventions are as in Figs. 1 and 2. Scale bar = 100 μm. For the insert, scale bar = 500 μm.

Are K pathway axons similar across primates?

The existence of three cell size classes of relay cells appears to be a ubiquitous feature of the mammalian LGN (Stone, 1983). However, in primates it could be argued that K LGN cells are not homologous across species, because, unlike P and M LGN cells, K cells vary in location in the LGN of different primates. Closer inspection of the K cell distributions suggests that what varies is the relative concentration of K cells within the different K layers. Viewed in this way, the K pathway is not that different from the P and M pathways which also exhibit species differences in degree of development and number of layers present (Kaas et al., 1978).

Other features of the K pathway also are common across primates. Although debated for macaque monkey LGN (Leventhal et al., 1981; Perry & Cowey, 1984), evidence indicates that K LGN cells in primates receive retinal input principally from a unique set of gamma-like small ganglion cells (Leventhal et al., 1981; Itoh et al., 1982; Conley & Fitzpatrick, 1989). Additionally, K cells receive a substantial input from the superficial layers of the superior colliculus and from the parabigeminal nucleus (Harting et al., 1991*a*,*b*). Recent evidence demonstrates that the K LGN cells not only receive inputs that are distinct from P and M LGN cells, but also are neurochemically distinct in calcium-binding protein con-

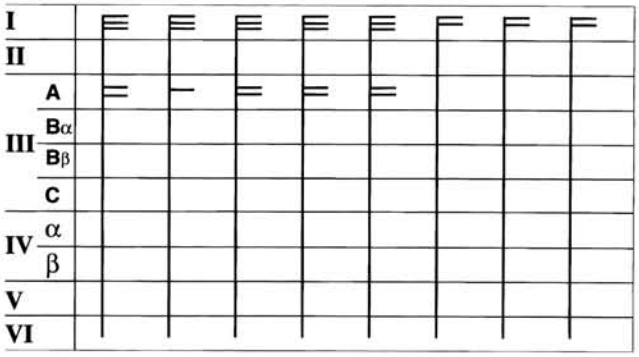

Fig. 11. A schematic diagram summarizing the branching patterns of the 8 axons reconstructed following LGN injections centered in layer K1. Conventions are as in Fig. 9.

tent and CO activity (Jones & Hendry, 1989; Johnson & Casagrande, 1993, 1995). Calbindin-D 28-kd immunoreactivity is dense, CO staining is light, and parvalbumin immunoreactivity is virtually absent in K LGN cell layers in all simian (including human) and prosimian primates examined (Jones & Hendry, 1989; Johnson & Casagrande, 1993, 1995; Hendry & Casagrande, 1996). In contrast, parvalbumin and CO immunoreactivity is dense in the P and M layers where little calbindin immunoreactivity is present (Jones & Hendry, 1989; Johnson & Casagrande, 1993, 1995). Finally, results of bulk labeling of the K pathway in a variety of New and Old World primates including owl monkeys (this paper), squirrel monkeys, macaque monkeys, *Cebus* monkeys, and bush babies demonstrate that the K pathway terminates separately from the M and P pathways in V1; K cells send axons supragranularly to cortical layers III and I of V1, while P and M cells send axons principally to granular layers IVα and IVβ (Casagrande & DeBruyn, 1982; Livingstone & Hubel, 1982; Fitzpatrick et al., 1983; Weber et al., 1983; Diamond et al., 1985; Hendry & Yoshioka, 1994; Casagrande, 1994). These findings are now further reinforced by the present data showing that the K axons in owl monkeys, as in the distantly related bush baby (Lachica & Casagrande, 1992), are morphologically distinct from the P and M LGN arbors. K axons in both species are thin and terminate as relatively small, delicate arbors focused within a single CO blob column. In contrast, P and M axons are thicker and terminate as more robust arbors that are not restricted to CO blob columns (Lachica & Casagrande, 1992; unpublished observations).

If the K pathway is actually made up of several subpathways (see also below), it could still be the case that the composition of the K pathway differs across species. Several differences between primate species in K pathway organization are noteworthy. In simian primates, the proportion of cells belonging to the K LGN pathway appears qualitatively to be smaller than in prosimians. This impression is likely the result of the relatively enormous increase in the number of P cells in some simians rather than in a quantitative difference in K LGN cells. In fact, counts of the LGN P, M and K cells in macaque monkeys have shown that K cells and M cells each account for a similar proportion (about 10% each) of the total population of cells in the LGN (Hendry, 1995). Similar counts have not been done in prosimians, but the qualitative impression is that K and M LGN cells are about equal in number. Another difference in K LGN cell anatomy between simians (e.g. macaque monkeys, owl monkeys, and squirrel monkeys) and prosimians (e.g. bush babies) is that in simians K LGN cells are often grouped into patches of cells between the P and M layers (see Fig. 1), whereas in prosimians the K LGN cells are mainly found in two specialized layers that appear as thin versions of the main P and M layers. A third difference in K LGN pathway organization between primates concerns the relative development of individual LGN K layers (see Hendry & Casagrande, 1996 and unpublished). In some, but not all, simian primates such as owl monkeys, squirrel monkeys, and macaque monkeys, the most prominent K layers are K1 and K3. In the prosimian bush baby, the most well-developed K population exists as two layers defined here as K4. Also, analysis of K axon morphology in bush babies shows that all K LGN arbors terminate within cortical layer III of V1 with collateral branches to layer I. In contrast, in owl monkeys the present results reveal a variety of K morphological axon types, some of which innervate only in layer III or only in layer I. One possibility, an issue we consider in more detail below, is that each K LGN layer contains a functionally unique population of cells. In that case the differences in K axon morphology between owl monkeys and bush babies may simply be a reflection of the fact that different K layers were studied in each case. Regardless, the relative differences in the number of K cells in the different K layers in different primate species hint that there may be functional specialization within the K pathway.

Do K axons belong to a single class?

Our results suggest that K axons in simians are morphologically diverse. Of particular interest is the finding that the major target of the majority of K1 cells in owl monkeys is cortical layer I. In contrast, the major target of the majority of K3 axons appears to be cortical layer IIIBα. These results for owl monkeys are in agreement with studies by Fitzpatrick et al. (1983) using bulk labeling of LGN or cortex in squirrel monkeys. They found evidence both from retrograde and anterograde labeling that the main projection to cortical layer III was from what they termed the internal intercalated layer (K3); the external intercalated layer (K1) as well as K2 appeared to account for the main projections to cortical layer I. Curiously, just the opposite results were reported for the same species (squirrel monkeys) by Weber et al. (1983), who claimed that what they termed the "S" layers (K1) had projections that terminated as patches within cortical layer III and that cells in the interlaminar zones above the S layers had projections to cortical layer I. These conflicting findings in squirrel monkeys might be attributed to misinterpretations of results of very large injections in the study of Weber et al. (1983). Resolution of these disagreements ultimately will require studies of the sort we have done here in the owl monkey in which individual axons are reconstructed following limited injections of K LGN layers in other monkeys. Regardless, all of these results support the idea that different K layers in simians have different projection patterns.

There are at least two problems with trying to determine if each K LGN layer gives rise to a distinct morphological axon type. The first problem is one of definition. If each population of axons is heterogeneous, what features will be used to distinguish the classes? Second, it is very difficult to label K layers individually due to their small size and still get a decent sample of axons. We encountered both of these problems in the current study of K axons in owl monkeys. Nevertheless, comparisons of axons labeled from injections centered in layer K3 with axons labeled from injections centered in K1 suggested that, in spite of within group heterogeneity, each set of axons represents a distinct group. All axons from the K1 injections arborize superficial to K3 axons and terminate principally in cortical layer I. All axons from the K3 injections arborize principally in cortical layer IIIBα, with a few axons having branches in layer I. Results of our retrograde studies hint that K4 axons may also be distinguishable from some K3 axons in not having an axon collateral to cortical layer I. Finally, our single labeled axon in V2 indicates that K axons that project to V2 may be quite distinct from those projecting to V1 with broad terminal arbors in layers IIIC and V. Clearly, a more detailed study designed to specifically target each K layer would be required to determine specific differences in K layer axon morphology for axons terminating in both V1 and V2.

Functional considerations

The vast majority of K axon boutons in owl monkey are found within a CO blob column of cortical layers IIIA/IIIB and IIIC. The direct projection of the K pathway to CO blob cells in these cortical layers potentially would allow the K pathway to influence cells projecting to V2 stripes, which in turn project to higher order

visual areas concerned with color or brightness contrast (Livingstone & Hubel, 1988; Krubitzer & Kaas, 1989). For the nocturnal owl monkey, a role in color vision seems less likely than a role in brightness contrast. Unfortunately, there are no studies that have examined K LGN cells physiologically in any simian primate so it is unclear what specific qualities would be contributed by K LGN cells. Physiological studies of these cells in bush babies suggest that a subpopulation of K cells could contribute to visual resolution based upon their contrast-sensitivity functions (Norton et al., 1988). The latter studies found that the K cells (those that could be driven by grating stimuli) have peak spatial frequency cutoffs and contrast sensitivities intermediate between those of the M and P cells.

Other characteristics of the K pathway, especially the connections from the superior colliculus, suggest a role for the K pathway in perception during eye movements (Casagrande, 1994). K cells could be visually driven either directly from the retina or indirectly from strong input from the colliculus (Harting et al., 1991*a*; Lachica & Casagrande, 1993; Feig & Harting, 1994). Many superficial collicular cells in macaque monkeys show an enhancement of response prior to a saccadic eye movement (Wurtz & Goldberg, 1972). The superior colliculus has also been shown to influence the response of the LGN cells in ways that suggest that this pathway could be involved with eye movements (Lal & Friedlander, 1990; Xue et al., 1994). Moreover, K axons can influence cortical cells within both of the major pathways to the extrastriate areas since, in addition to the projections associated with the "form pathway," some K axons in owl monkeys have side branches that terminate in cortical layer IIIC. Cells in IIIC project directly to area MT, an area that has been implicated in the perception of motion (Newsome & Pare, 1988; Krubitzer & Kaas, 1990; Kaas & Morel, 1993; Merigan & Maunsell, 1993). Also, the K pathway could contribute to aspects of eye movements *via* another pathway, namely to the dorsomedial visual area (DM). CO blobs in V1 in owl monkeys and other primates project strongly to DM (Krubitzer & Kaas, 1993). DM, in turn, projects most heavily to ventral posterior parietal area (VPP, ventral intraparietal area [VIP] of macaque monkeys), as well as to other areas such as MT which are associated with eye movements. Thus far, it has been unclear what role the pathway from CO blobs to DM plays. Perhaps this channel to the extrastriate areas carries signals dominated by the K pathway in the same manner as it has been suggested that the pathway from V1 to MT is dominated by the M channel (Merigan & Maunsell, 1993).

Another suggestion for a role for the K pathway is that it plays a modulatory role (Casagrande, 1994). Thalamic pathways that target cortical layer I are often suggested to be modulatory pathways given the physiological evidence that cortical layer I plays such a role (Vogt, 1991). Certainly the major projection of the K1 axons, as well as collaterals of some K3 axons of owl monkeys to cortical layer I, are supportive of such a proposal. Such a proposal also harks back to suggestions by Stone (1983) that a comparable pathway, the W-cell pathway, is important for ambient as opposed to focal vision.

A final possibility is that given the diversity of axon morphology of K axons in owl monkeys, K pathway axons have multiple roles of which the above are some likely candidates. Further research on the anatomical and physiological properties of K cells will be required to move beyond broad speculation of the K pathway's functional role in vision. To fully appreciate how information from the K pathway is utilized at that cortical level, studies on whether and how the three parallel visual streams mix signals in the CO blobs of V1 are needed. These pathways appear to arise from separate groups of retinal ganglion cells, remain segregated in the LGN as the P, M, and K layers, and persist as separate populations up to the first synapse, but projections intermix beyond the first synapse. Aspects of the role or roles of the K pathway also might be revealed by direct examination of the response properties of K cells in awake animals or by analysis of the effects of manipulating all three parallel pathways independently.

Acknowledgments

We thank Ms. J. Mavity-Hudson and Dr. J. Boyd for help with processing the tissue and making figures. We greatly appreciate the very useful comments on the manuscript provided by Drs. J. Boyd, S. Hendry, J. Schall, J. Kaas, and M. Powers, as well as Ms. A. Wiencken and Ms. J. Mavity-Hudson. This research was supported by NEI Grant EY01778 (to V.A. Casagrande) and core grants EY08126 and HD15052.

References

Allman, J.M. & Kaas, J.H. (1971). Representation of the visual field in striate and adjoining cortex of the owl monkey (*Aotus trivirgatus*). *Brain Research* **35**, 89–106.

Benevento, L.A. & Yoshida, K. (1981). The afferent and efferent organization of the lateral geniculo-prestriate pathways in the macaque monkey. *Journal of Comparative Neurology* **203**, 455–474.

Boyd, J.D., Mavity-Hudson, J.A. & Casagrande, V.A. (1997). Projection of layer IV to layer III in striate cortex of owl monkey (in preparation).

Brodmann, K. (1909). Vergleichende Lokalisationlehre der Grosshirnrinde in ihren Prinzipien dargestellt auf Grund des Zellenbaues. J.A. Barth, Leipzig.

Bullier, J. & Kennedy, H. (1983). Projection of the lateral geniculate nucleus onto cortical area V2 in the macaque monkey. *Experimental Brain Research* **53**, 168–172.

Campos-ortega, J.A. & Hayhow, W.A. (1970). A new lamination pattern in the lateral geniculate nucleus of primates. *Brain Research* **20**, 335–339.

Casagrande, V.A. (1994). A third parallel visual pathway to primate area V1. (Review). *Trends in Neuroscience* **17**, 305–310.

Casagrande, V.A. & DeBruyn, E.J. (1982). The galago visual system: Aspects of normal organization and developmental plasticity. In *The Lesser Bush Baby (Galago) An Animal Model: Selected Topics*, ed. Haines, D.E., pp. 138–162. Boca Raton, Florida: CRC Press.

Casagrande, V.A. & Kaas, J.H. (1994). The afferent, intrinsic, and efferent connections of primary visual cortex. In *Cerebral Cortex, Vol. 10, Primary Visual Cortex of Primates*, ed. Peters, A. & Rockland, K., pp. 201–259. New York: Plenum Press.

Chacko, L.W. (1955). The lateral geniculate body in gibbon (*Hylobates hoolock*). *Journal of the Anatomical Society of India* **4**, 69–81.

Conley, M. & Fitzpatrick, D. (1989). Morphology of retinogeniculate axons in the macaque. *Visual Neuroscience* **2**, 287–296.

Diamond, I.T., Conley, M., Itoh, K. & Fitzpatrick, D. (1985). Laminar organization of geniculocortical projections in *Galago senegalensis* and Aotus trivirgatus. *Journal of Comparative Neurology* **242**, 584–610.

Diamond, I.T., Fitzpatrick, D. & Schmechel, D. (1993). Calcium binding proteins distinguish large and small cells of the ventral posterior and lateral geniculate nuclei of the prosimian galago and the tree shrew (*Tupaia balangeri*). *Proceedings of the National Academy of Sciences of the U.S.A.* **90**, 1425–1429.

Feig, S. & Harting, J.K. (1994). Ultrastructural studies of the primate lateral geniculate nucleus: Morphology and spatial relationships of axon terminals arising from the retina, visual cortex (area 17), superior colliculus, parabigeminal nucleus, and pretectum of *Galago crassicaudatus*. *Journal of Comparative Neurology* **343**, 17–34.

Fitzpatrick, D., Itoh, K. & Diamond, I.T. (1983). The laminar organization of the lateral geniculate body and the striate cortex in the squirrel monkey (*Saimiri sciureus*). *Journal of Neuroscience* **3**, 673–702.

Gibson, A.R., Hansma, D.I., Houk, J.C. & Robinson, F.R. (1984). A sensitive low artifact TMB procedure of the demonstration of WGA-HRP in the CNS. *Brain Research* **298**, 235–241.

Giolli, R.A. & Tigges, J. (1970). The primary optic pathways and nuclei in primates. In *Advances in Primatology, Vol. 1*, ed. Noback, C.R. & Montagna, W., pp. 29–54. New York: Appleton-Century-Crofts.

HARTING, J.K., HUERTA, M.F., HASHIKAWA, T. & VAN LIESHOUT, D.P. (1991*a*). Projection of the mammalian superior colliculus upon the dorsal lateral geniculate nucleus: Organization of tectogeniculate pathways in nineteen species. (Review). *Journal of Comparative Neurology* **304**, 275–306.

HARTING, J.K., VAN LIESHOUT, D.P., HASHIKAWA, T. & WEBER, J.T. (1991*b*). The parabigeminogeniculate projection: Connectional studies in eight mammals. *Journal of Comparative Neurology* **305**, 559–581.

HÄSSLER, R. (1967). Comparative anatomy of central visual systems in day- and night-active primates. In *Evolution of the Forebrain*, ed. HÄSSLER, R. & STEPHAN H., pp. 419–434. New York: Plenum Press.

HENDRY, S.H.C. (1995). A neurochemically distinct pathway. In *Thalamic Networks for Relay and Modulation*, ed. MINCIACCHI, M., MOLINARI, M., MACCHI, G. & JONES, E.G., pp. 251–267. New York: Pergamon Press.

HENDRY, S.H.C. & CASAGRANDE, V.A. (1996). A common pattern for a third visual channel in the primate LGN. *Society for Neuroscience Abstracts* **22**, 1605.

HENDRY, S.H. & YOSHIOKA, T. (1994). A neurochemically distinct third channel in the macaque dorsal lateral geniculate nucleus. *Science* **264**, 575–577.

HERNANDEZ-GONZALEZ, A., CAVADA, C. & REINOSO-SUAREZ, F. (1994). The lateral geniculate nucleus projects to the inferior temporal cortex in the macaque monkey. *Neuroreport* **5**, 2993–2996.

IRVIN, G.E., NORTON, T.T., SESMA, M.A. & CASAGRANDE, V.A. (1986). W-like response properties of interlaminar zone cells in the lateral geniculate nucleus of a primate (*Galago crassicaudatus*). *Brain Research* **362**, 254–270.

ITOH, K., CONLEY, M. & DIAMOND, I.T. (1982). Retinal ganglion cell projections to individual layers of the lateral geniculate body in *Galago crassicaudatus*. *Journal of Comparative Neurology* **205**, 282–290.

JOHNSON, J.K. & CASAGRANDE, V.A. (1993). Calcium-binding protein expression correlates with primate visual parallel pathways. *Society for Neuroscience Abstracts* **19**, 425.

JOHNSON, J.K. & CASAGRANDE, V.A. (1995). Distribution of calcium-binding proteins within the parallel visual pathways of a primate (*Galago crassicaudatus*). *Journal of Comparative Neurology* **356**, 238–260.

JONES, E.G. & HENDRY, S.H.C. (1989). Differential calcium-binding protein immunoreactivity distinguishes classes of relay neurons in the monkey thalamic nuclei. *European Journal of Neuroscience* **1**, 222–246.

KAAS, J.H., LIN, C.S. & CASAGRANDE, V.A. (1976). The relay of ipsilateral and contralateral retinal input from the lateral geniculate nucleus to striate cortex in the owl monkey: A transneuronal transport study. *Brain Research* **106**, 371–378.

KAAS, J.H. & MOREL, A. (1993). Connections of visual areas of the upper temporal lobe of owl monkeys: The MT crescent and dorsal and ventral subdivisions of FST. *Journal of Neuroscience* **13**, 534–546.

KAAS, J.H., HUERTA, M.F., WEBER, J.J., & HARTING, J.K. (1978). Patterns of retinal terminations and laminar organization of the lateral geniculate nucleus of primates. *Journal of Comparative Neurology* **182**, 517–554.

KENNEDY, H. & BULLIER, J. (1985). A double-labeling investigation of the afferent connectivity to cortical areas V1 and V2 of the macaque monkey. *Journal of Neuroscience* **5**, 2815–2830.

KRUBITZER, L.A. & KAAS, J.H. (1989). Cortical integration of parallel pathways in the visual system of primates. *Brain Research* **478**, 161–165.

KRUBITZER, L.A. & KAAS, J.H. (1990). Cortical connections of MT in four species of primates: Areal, modular, and retinotopic patterns. (Review). *Visual Neuroscience* **5**, 165–204.

KRUBITZER, L.A. & KAAS, J.H. (1993). The dorsomedial visual area of owl monkeys: Connections, myeloarchitecture, and homologies in other primates. *Journal of Comparative Neurology* **334**, 497–528.

LACHICA, E.A. & CASAGRANDE, V.A. (1992). Direct W-like geniculate projections to the cytochrome oxidase (CO) blobs in primate visual cortex: Axon morphology. *Journal of Comparative Neurology* **319**, 141–158.

LACHICA, E.A. & CASAGRANDE, V.A. (1993). The morphology of collicular and retinal axons ending on small relay (W-like) cells of the primate lateral geniculate nucleus. *Visual Neuroscience* **10**, 403–418.

LAL, R. & FRIEDLANDER, M.J. (1990). Effect of passive eye movement on retinogeniculate transmission in the cat. *Journal of Neurophysiology* **63**, 523–38.

LEVENTHAL, A.G., RODIECK, R.W. & DREHER, B. (1981). Retinal ganglion cell classes in the Old World monkey: Morphology and central projections. *Science* **213**, 1139–1142.

LIVINGSTONE, M.S. & HUBEL, D.H. (1982). Thalamic inputs to cytochrome oxidase-rich regions in monkey visual cortex. *Proceedings of the National Academy of Sciences of the U.S.A.* **79**, 6098–6101.

LIVINGSTONE, M.S. & HUBEL, D.H. (1988). Segregation of form, color, movement, and depth: Anatomy, physiology, and perception. *Science* **240**, 740–749.

LUND, J.S. (1988). Anatomical organization of macaque monkey striate visual cortex. (Review). *Annual Review of Neuroscience* **11**, 253–288.

LYSAKOWSKI, A., STANDAGE, G.P. & BENEVENTO, L.A. (1988). An investigation of collateral projections of the dorsal lateral geniculate nucleus and other subcortical structures to cortical areas V1 and V4 in the macaque monkey: A double label retrograde tracer study. *Experimental Brain Research* **69**, 651–661.

MERIGAN, W.H. & MAUNSELL, J.H. (1993). How parallel are the primate visual pathways? (Review). *Annual Review of Neuroscience* **16**, 369–402.

NEWSOME, W.T. & PARE, E.B. (1988). A selective impairment of motion perception following lesions of the middle temporal visual area (MT). *Journal of Neuroscience* **8**, 2201–2211.

NORTON, T.T. & CASAGRANDE, V.A. (1982). Laminar organization of receptive-field properties in lateral geniculate nucleus of bush baby (*Galago crassicaudatus*). *Journal of Neurophysiology* **47**, 715–741.

NORTON, T.T., CASAGRANDE, V.A., IRVIN, G.E., SESMA, M.A. & PETRY, H.M. (1988). Contrast-sensitivity functions of W-, X-, and Y-like relay cells in the lateral geniculate nucleus of bush baby, *Galago crassicaudatus*. *Journal of Neurophysiology* **59**, 1639–1656.

PERRY, V.H. & COWEY, A. (1984). Retinal ganglion cells that project to the superior colliculus and pretectum in the macaque monkey. *Neuroscience* **12**, 1125–1137.

SAWCHENKO, P.E., CUNNINGHAM, E.T., JR., MORTRUD, M.T., PFEIFFER, S.W. & GERFEN, C.R. (1990). *Phaseolus vulgaris leucoagglutinin* anterograde axonal transport technique. In *Methods in Neuroscience, Vol. 3*, ed. CONN, M., pp. 247–260. San Diego, California: Academic Press.

STONE, J. (1983). *Parallel Processing in the Visual System: The Classification of Retinal Ganglion Cells and Its Impact on the Neurobiology of Vision*. New York: Plenum Press.

VOGT, B.A. (1991). The role of layer I in cortical function. In *Cerebral Cortex: Normal and Altered States of Function, Vol. 9*, ed. PETERS, A. & JONES, E.G., pp. 49–80. New York and London: Plenum Press.

WEBER, J.T., HUERTA, M.F., KAAS, J.H. & HARTING, J.K. (1983). The projections of the lateral geniculate nucleus of the squirrel monkey: Studies of the interlaminar zones and the S layers. *Journal of Comparative Neurology* **213**, 135–145.

WONG-RILEY, M.T. (1979). Projections from the dorsal lateral geniculate nucleus to prestriate cortex in the squirrel monkey as demonstrated by retrograde transport of horseradish peroxidase. *Brain Research* **109**, 595–600.

WURTZ, R.H. & GOLDBERG, M.E. (1972). Activity of superior colliculus in behaving monkey. IV. Effects of lesions on eye movements. *Journal of Neurophysiology* **35**, 587–596.

XUE, J.T., KIM, C.B., MOORE, R.J. & SPEAR, P.D. (1994). Influence of the superior colliculus on responses of lateral geniculate neurons in the cat. *Visual Neuroscience* **11**, 1059–1076.